

Preparation of π -Conjugated Polymers Composed of Hydroquinone, *p*-Benzoquinone, and *p*-Diacetoxyphenylene Units. Optical and Redox Properties of the Polymers

Takakazu Yamamoto,* Tohru Kimura, and Kouichi Shiraishi

Research Laboratory of Resources Utilization, Tokyo Institute of Technology, 4259 Nagatsuta, Midori-ku, Yokohama 226-8503, Japan

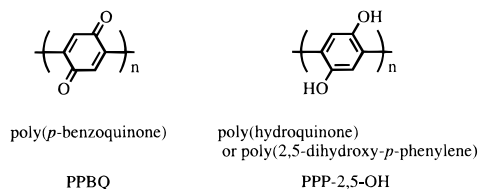
Received May 19, 1999

ABSTRACT: π -Conjugated poly(hydroquinone)s and poly(*p*-benzoquinone)s have been prepared, and their optical and redox behaviors have been studied. Poly(hydroquinone-2,5-diyl), PPP-2,5-OH, with a weight-average molecular weight of 8500 (determined by the light scattering method) was soluble in DMF. The π - π^* absorption peak of hydroquinone at 296 nm is shifted to 345 nm in PPP-2,5-OH. PPP-2,5-OH underwent electrochemical two-step oxidation at about 0.5 and 0.8 V versus Ag/Ag⁺. Another type of poly(*p*-hydroquinone)s in an acetylenic main chain was also prepared, and the polymer underwent oxidation with the first oxidation peak at about 1.0 V versus Ag/Ag⁺. Optical and X-ray diffraction data of the polymers and their precursor polymers suggest stacking of the polymer molecules.

Introduction

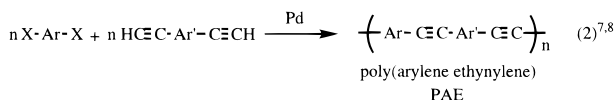
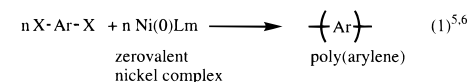
π -Conjugated polymers constituted of redox-active units are the subject of many recent papers.¹ Quinones and hydroquinones belong to typical redox-active species, and their chemical behavior has been extensively studied.² However, examples of well-characterized main-chain-type polyquinones and investigation of their redox behavior have been limited.³

p-Benzoquinone is the simplest quinone, and revealing the chemical properties of the following benzoquinone and hydroquinone polymers is considered interesting.

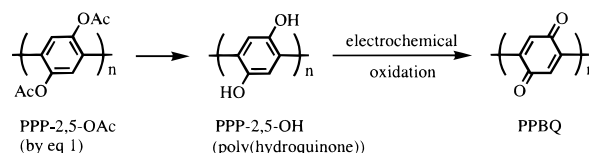


Dordick and co-workers^{3a} reported the preparation of meta-bonded poly(hydroquinone) and its interesting electrochemical response. Yamamoto and co-workers⁴ reported the preparation of a film of poly(dihydroxyphenylene) (or poly(hydroquinone)) by electrooxidative polymerization of hydroquinone. However, in this case, the bonding mode between the monomeric units in the polymer is not controlled (e.g., the polymer may contain 1,2-bonding⁴), and the preparation of soluble poly(hydroquinone) by electrochemical polymerization has not been reported.

On the other hand, recently developed organometallic polycondensation^{5–8} of dihaloaromatic compounds $X-Ar-X$ gives π -conjugated polymers with well-characterized bonds.



Application of the polycondensation expressed by eq 1 to 2,5-diacetoxy-*p*-dihalobenzene (as $X-Ar-X$) gives the following precursor π -conjugated polymers, PPP-2,5-OAc, that can be converted into the main-chain-type poly(hydroquinone) and poly(*p*-benzoquinone).



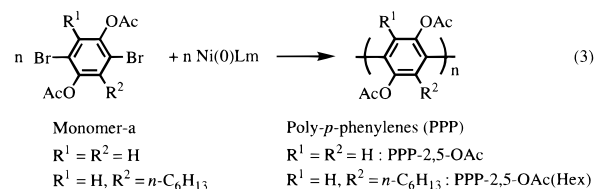
Solubility of the PPP-2,5-OH shown above can be controlled by the kind of solvent used, and studies on the redox behavior of PPP-2,5-OH both in the solid state (film) and in solutions become possible.

An acetylenic polymer containing the hydroquinone unit ($-Ar- = \text{hydroquinone unit: } -p-C_6H_2(OH)_2-$) has also been obtained through eq 2.

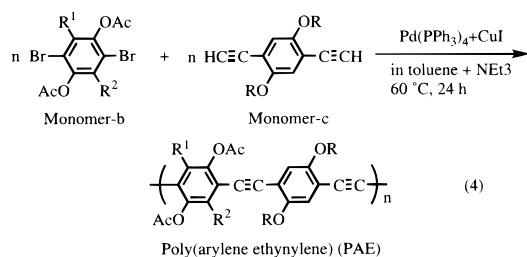
Herein, we report the preparation of these two kinds of redox-active polymers and their optical and redox properties. Electrochemical responses of molecules having a large π -conjugation system and polymer-modified electrodes have been the subject of many recent papers.⁹ The electrochemical behavior of non- π -conjugated polymers of quinone^{10a,b} and its analogue (tetracyanoquinodimethane)^{10c,d} has been reported.

Results and Discussion

Preparation of Polymers with Diacetoxy-*p*-phenylene Unit. Polymers containing the 2,5-diacetoxy-*p*-phenylene unit were prepared according to the following reaction:



The following polymers were also prepared:



$R^1 = R^2 = H$, $R = n\text{-OC}_{12}\text{H}_{25}$: PAE-1

$R^1 = R^2 = H$, $R = n\text{-OC}_6\text{H}_{13}$: PAE-2

$R^1 = R^2 = \text{CN}$, $R = n\text{-OC}_{12}\text{H}_{25}$: PAE-3

$R^1 = R^2 = \text{CN}$, $R = n\text{-OC}_6\text{H}_{13}$: PAE-4

$\text{Pd}(\text{PPh}_3)_4$ = tetrakis(triphenylphosphine)palladium(0)

These polymerization gave the corresponding polymers in 72–100% yield. Table 1 summarizes the results of the polymerizations.

For the zerovalent nickel complex, $\text{Ni}(0)\text{L}_m$, a mixture of bis(1,5-cyclooctadiene)nickel(0) and 2,2'-bipyridyl was used in DMF.⁵ Thus, PPP-2,5-OAc was obtained. The polymer showed a M_n value of 3400 ($M_w/M_n = 1.6$) in the GPC analysis (polystyrene standards), although the polymer may have a strong interaction with the GPC column and the GPC analysis may give a seemingly lower molecular weight than a real molecular weight. PPP-2,5-OH prepared by hydrolysis of PPP-2,5-OAc showed a higher molecular weight in its light scattering analysis (vide infra).

The molecular weight of PPP-2,5-OAc obtained in the GPC analysis is comparable to that observed with polypyridine ($M_w = 4300$)^{6f} prepared analogously. The precipitation of the polymer may prevent further elongation of the polymer chain, although it has been reported that Ni-promoted organometallic polycondensations give polymers with higher molecular weights when applied to the preparation of alkylated or alkoxyalkylated π -conjugated polymers. Thus, the polycondensations have given π -conjugated poly(alkylpyridine)s ($M_w = 12\,000\text{--}36\,000$),^{6f} poly(alkylthiophene)s ($M_n = 26\,000\text{--}35\,000$),¹¹ poly(alkylthiazole)s (M_n or $M_w = 11\,000\text{--}21\,000$),^{6d,e,11f,12a} and poly(alkylquinoxaline)s ($M_w = 14\,000\text{--}44\,000$)^{12b} with higher molecular weights.

The monomer with a hexyl group ($R^1 = H$, $R^2 = \text{hexyl}$), however, gave only an oligomeric product in the present polymerization, presumably due to a large steric repulsion between the monomeric units. Use of the monomers with $R^1 = R^2 = n\text{-C}_6\text{H}_{13}$ and $R^1 = R^2 = \text{CN}$ in eq 3 gave analogous results.

The phenyl-OAc bond sometimes oxidatively adds to the $\text{Ni}(0)$ complexes to be cleaved.¹³ However, in the present polymerization expressed by eq 3, the phenyl-Br bond seems to have a much higher reactivity toward $\text{Ni}(0)\text{L}_m$ than does the phenyl-OAc bond, and hence, the phenyl-OAc bond remains intact.

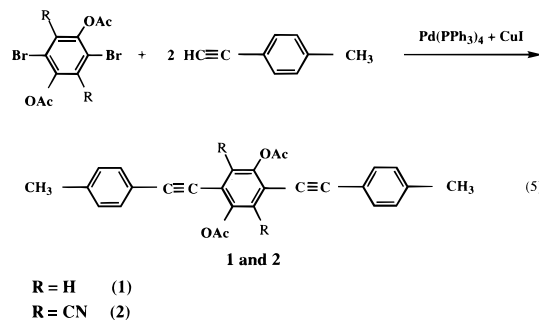
The IR and ^1H NMR spectra (cf. Supporting Information) and data from elemental analysis agree with the proposed structure of PPP-2,5-OAc.¹⁴ The IR spectrum of PPP-2,5-OAc resembles that of monomer a ($R^1 = R^2 = H$), except for the disappearance of the $\nu(\text{C}-\text{Br})$ band of the monomer a at 1060 cm^{-1} after the polymerization. The peak area ratio between the OAc and aromatic protons in the ^1H NMR spectrum is consistent with the structure of the polymer, although the peaks appear as a multiplet, suggesting the presence of rotamers.¹⁴ PPP-2,5-OAc is soluble in chloroform, DMF, and DMSO and partly soluble in toluene and THF; however, it is not soluble in methanol.

Table 1. Preparation of Polymers Having the 2,5-Diacetoxy-*p*-phenylene Unit^a or Benzodithiophene Unit

run	monomer ^b			solvent ^c	yield	<i>M</i> _n (<i>M</i> _w / <i>M</i> _n) ^d
	R ¹	R ²	R in OR			
polymerization according to eq 3						
1	H	H		DMF	72	3400 (1.6)
2	H	hex		DMF	100	530 (1.2)
polymerization according to eq 4 ^e						
3	H	H	dod	C ₇ H ₈ + NEt ₃	89	7000 (1.7) ^f
4	H	H	hex	C ₇ H ₈ + NEt ₃	96	4600 (2.3) ^f
5	CN	CN	dod	C ₇ H ₈ + NEt ₃	84	^g
6	CN	CN	hex	C ₇ H ₈ + NEt ₃	98	2400 (1.5) ^f

^a At 60 °C for 24 h. ^b Key: hex = hexyl, oct = octyl, dec = decyl, and dod = dodecyl. ^c C_7H_8 = toluene. ^d Determined by GPC (vs polystyrene standards). Eluent = DMF for runs 1 and 2; CHCl_3 for runs 3–5. ^e At a lower temperature or a shorter reaction time, only oligomeric products were obtained, as judged from their UV-vis spectra. ^f For the CHCl_3 -soluble part. ^g Not measured.

The polymerization expressed by eq 4 proceeded smoothly at 60 °C to give PAE-type polymers (runs 3–6 in Table 1). The following model reaction also gave compounds **1** and **2** in good yields. IR spectra of the



model compounds and the PAE-type polymers showed a $\nu(\text{C}=\text{O})$ band at about 1750 (**1** and PAE-1) or 1780 cm^{-1} (**2** and PAE-3) and a $\nu(\text{C}\equiv\text{C})$ band at about 2200 cm^{-1} . Their strong $\nu(\text{C}\equiv\text{N})$ bands for **2** and PAE-3 overlap the $\nu(\text{C}\equiv\text{C})$ band. Polymers PAE-1–4 showed only low solubility in organic solvents. They were only partly soluble in chloroform, DMF, NMP, and carbon disulfide, and the chloroform-soluble parts exhibited M_n values of 2400–7000 (runs 3–5 in Table 1), as determined by GPC (polystyrene standards). The molecular weights of the soluble parts were lower than those of previously reported PAE-type polymers.^{7b,c,8} The insoluble parts are considered to have higher molecular weights and possess essentially the same molecular structures as those of the soluble parts because both of them show the same IR spectra. The low solubility of the polymers is considered to arise from a strong CT packing interaction, which is discussed below. Occurrence of Glaser-type oxidative coupling¹⁵ between the acetylenic monomers (monomer c) or oligomers is unlikely because the polymerization was carried out under an atmosphere of nitrogen. Formation of an ordered structure, as judged from powder X-ray diffraction patterns of the polymers, supports this view (vide infra).

Figure 1 shows the molecular structure of model compound **1** as determined by X-ray crystallography. The molecule adopts the linear and coplanar structure, and the $\text{C}(8)\text{--C}(9)$ distance (1.16 \AA) is normal for the $\text{C}\equiv\text{C}$ triple bond.

PPP-2,5-OAc (eq 3) did not contain halogen, indicating that they are H-terminated, similar to poly(anthraqui-

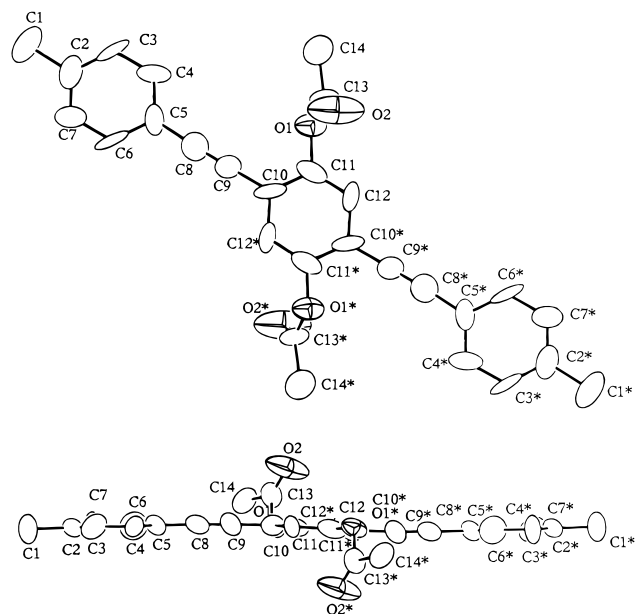


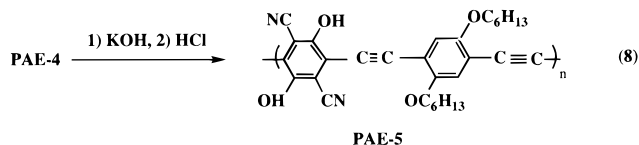
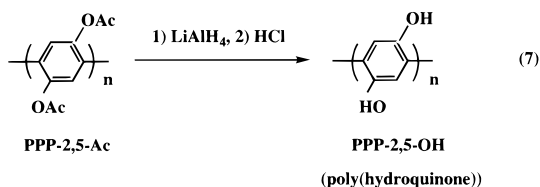
Figure 1. Molecular structure of the model compound **1**. Views from two directions are depicted. Selected bond lengths (Å) and angle (deg): O(1)–C(11) 1.40(1); O(2)–C(13) 1.14; C(5)–C(8) 1.44(2); C(8)–C(9) 1.16(1); C(9)–C(10) 1.45(2); C(1)–C(2) 1.51(1); C(13)–C(14) 1.50(2); C(11)–O(1)–C(13) 116.1(10); C(1)–C(2)–C(7) 123(1); C(4)–C(5)–C(6) 116(1); C(6)–C(5)–C(8) 119(1); C(8)–C(9)–C(10) 177; C(9)–C(10)–C(12) 116(1); O(1)–C(11)–C(10) 113(1); O(1)–C(13)–O(2) 123(1); O(2)–C(13)–C(14) 127(10); C(4)–C(5)–C(8) 124(1); C(5)–C(8)–C(9) 177(1); C(9)–C(10)–C(11) 124(1).

none)s^{3b} and poly(pyridine-2,5-diyl)^{5,6f} prepared by analogous methods. The H-terminated unit is considered to be formed by acidolysis of an Ni-terminated unit during the workup of the polymer:



The nickel compound formed in the polymerization was removed by treating the polymer with ethylenediaminetetraacetate (cf. the Experimental Section). Nickel compounds that might remain in the polymer were not detected. If the polymer contained a significant amount of paramagnetic^{16a} NiX₂(bpy), the ¹H NMR spectrum of PPP-2,5-OAc was considered to be broadened. However, the ¹H NMR peaks of PPP-2,5-OAc were sharp (cf. Supporting Information). A test with dimethylglyoxime^{16b} did not detect nickel in a burned sample of PPP-2,5-OAc. It was recently found that polypyridine^{6f} prepared by analogous Ni(0)Lm-promoted polycondensation contained 13 ppm of nickel after reprecipitation.^{16c} Powder X-ray diffraction pattern of PPP-2,5-OAc showed three peaks at *d* = 11.1, 4.90, and 4.03 Å. In contrast to the case of PPP-2,5-OAc, the PAE-type polymers contained terminal Br, as is usually observed with similar PAE-type polymers.^{7c,8b,d}

Transformation of OAc to OH. The OAc group in PPP-2,5-OAc and PAE-4 is readily transformed into the OH group via reactions with LiAlH₄¹⁷ and KOH, respectively. The ν(C=O) band of the original polymers completely disappears after the reactions. The OAc group in the PAE-type polymer can be hydrolyzed to the OH group (eq 8). The hydrolysis seems to proceed more easily with PAE-3, PAE-4, and **2** with the electron-withdrawing CN group, as is usually observed in organic chemistry (cf. the Experimental Section). Data from elemental analysis indicate that PPP-2,5-OH is obtained



as a hydrate (C₆H₄O₂·H₂O)_n. The IR spectrum of PPP-2,5-OH essentially agrees with that of poly(dihydroxyphenylene)⁴ prepared by electrochemical oxidation of hydroquinone. The ¹H NMR spectrum of PPP-2,5-OH in DMF-*d*₇ is also reasonable for the structure exhibited above and shows a multiplet¹⁴ at about δ 9 for the OH group. The OH signal shows a temperature-dependent shift characteristic of the hydrogen-bonded OH group (cf. the Experimental Section).

PPP-2,5-OH is soluble in DMF (about 20 mg/mL) and partly soluble in DMSO. However, it is insoluble in chloroform, CH₃CN, toluene, THF, and methanol.

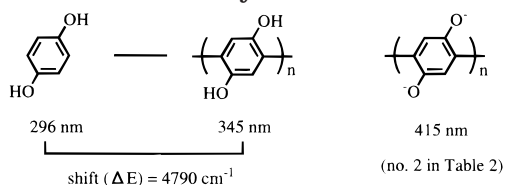
The GPC trace (in DMF) of PPP-2,5-OH gives *M*_n and *M*_w (weight-average molecular weight) of 3400 and 4800 (polystyrene standards), respectively, and light scattering analysis (in DMF with He–Ne laser (632.8 nm)) reveals that it has a larger *M*_w of 8500. Because PPP-2,5-OH does not show absorbance at the wavelength of the irradiated He–Ne laser and π-conjugated polymers give a large refractive index increment,^{6f,16d} the *M*_w value obtained in the light scattering analysis is reliable. The lower *M*_w given in the GPC analysis may be due to a strong interaction of PPP-2,5-OH with the GPC column. In DMF, PPP-2,5-OH shows an [η] value of 0.12 dL g^{−1}. Because of the controllability of the solubility of PPP-2,5-OH by changing the solvent, studies of its redox behaviors both in solutions and in the solid state (film) become possible.

UV–vis and Photoluminescence Data. PPP-2,5-OH. The π–π* absorption peak of hydroquinone¹⁸ is shifted to a longer wavelength region in the polymer, due to the expansion of the π-conjugation system (see Chart 1). UV–vis and photoluminescence data of the polymers are given in Table 2.

Addition of NaOH leads to the formation of salts of the polymer, and the UV–vis spectrum of PPP-2,5-OH continuously changes with increasing concentration of NaOH in DMF (cf. Supporting Information), showing an intermediate peak at 382 nm.^{19a} Finally, PPP-2,5-OH in alkaline DMF gives a peak at 415 nm (no. 2 in Table 2) that is assigned to a dianion species of PPP-2,5-OH.

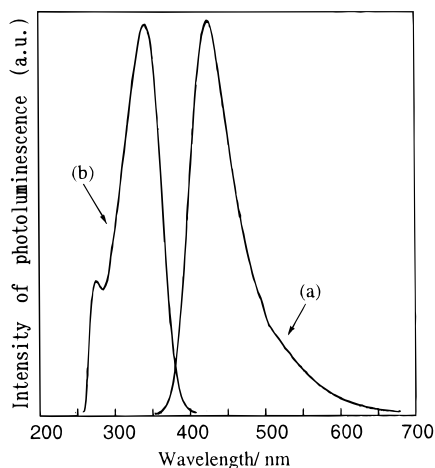
In air, the dianion species of PPP-2,5-OH is unstable, similar to dianion of hydroquinones^{19b} and gives peaks at 323, 380, and 500 nm at an early stage of oxidation in air. However, at the neutral state, PPP-2,5-OH was rather stable.

Figure 2 exhibits photoluminescence and excitation spectra of PPP-2,5-OH in DMF. The photoluminescence peak appears near the onset position (ca. 420 nm) of the π–π* absorption band of PPP-2,5-OH, as usually observed with π-conjugated polymers.^{6f,7b} The excitation spectrum essentially agrees with the absorption spectrum of PPP-2,5-OH (cf. Supporting Information). How-

Chart 1. Absorption Peaks of Hydroquinone and Polymers**Table 2. UV-Vis and Photoluminescence Data of the Polymers**

#	polymer	λ_{max} (nm)	photoluminescence	
			λ_{ph} (nm) ^a	quantum yield (%)
1	PPP-2,5-OAc	325, ^b 380 ^b (DMF)		
2	PPP-2,5-OH	345 (DMF) 415 (DMF/NaOH) 331 (film)	420 (DMF)	
3	PAE-1	418 (CHCl ₃) 470, 503 (film)	455, 490 ^c (CHCl ₃)	25
4	PAE-2	417 (CHCl ₃) 470, 510 (film)	458, 485 ^c (CHCl ₃)	29
5	PAE-3	500, 564 (CHCl ₃) ^d 492, 535 (film)	530, 580 ^c (CHCl ₃)	31
6	PAE-4	511, 570 (CHCl ₃) 500, 570 (film)	539, 580 ^c (CHCl ₃)	41
7	PAE-5	475 (NMP) 447 (film)	559 (NMP)	

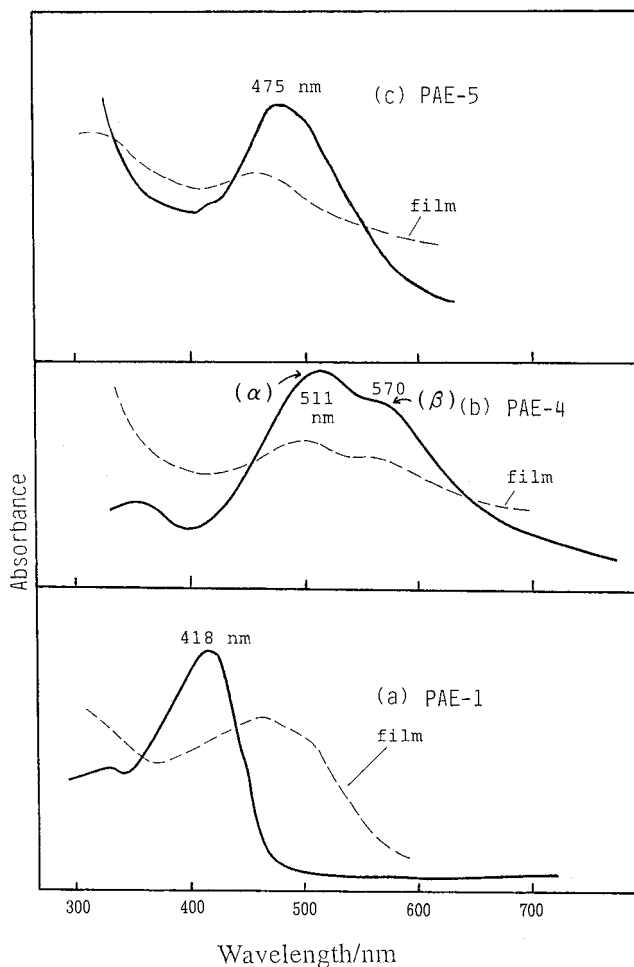
^a λ_{ph} = peak wavelength of the photoluminescence. ^b Shoulder peak. ^c Shoulder peak. ^d Essentially the same spectrum is obtained in DMF.

**Figure 2.** Photoluminescence spectrum of PPP-2,5-OH in DMF: (a) wavelength of irradiated light = 342 nm and (b) excitation spectrum monitored at 419 nm. Irradiation with 277 nm light gives essentially the same photoluminescence spectrum.

ever, it shows a shoulder peak at about 280 nm, which seems to be related to the absorption by a single hydroquinone unit (cf. Chart 1). Irradiation of PPP-2,5-OH with 277 nm light also leads to emission of light at 420 nm, suggesting occurrence of energy transfer from the photoactivated monomeric unit to the main-chain π -conjugated system, as sometimes observed with π -conjugated polymers.^{5c,20}

PAE-Type Polymers. Figure 3 shows UV-vis spectra of the PAE-type polymers. The peak position of the π - π^* absorption band of PAE-1 (λ_{max} = 418 nm; part a of Figure 3) is comparable to those of previously reported PAE-type polymers ($\text{ArC}\equiv\text{CAr}'\text{C}\equiv\text{C}$)_n.^{7,8,21}

Usual PAE-type polymer films give π - π^* absorption peaks at essentially the same position as those of their

**Figure 3.** UV-vis spectra for (a) PAE-1, (b) PAE-4, and (c) PAE-5. —: in solution (CHCl₃ for PAE-1 and -4 and NMP for PAE-5). - - -: in the solid state (film).

solutions. However, the film of PAE-1, which has long alkoxy side chains, shows two π - π^* absorption peaks²² at considerably longer wavelength regions. Recently, an analogous bathochromic shift has been observed with regioregular π -conjugated poly(3-alkylthiophene)s with long alkyl side chains^{11f,23,24} and this has been attributed to stacking of the polymer molecules in the solid state.

Similar stacking of coplanar PAE-1, assisted by the long OR side chain and interchain CT interaction, is conceivable. PAE-1 contains both electron-accepting p -C₆H₂(OAc)₂ and electron-donating p -C₆H₂(OR)₂, and the following stacking mode (Chart 2) having an intermolecular CT interaction^{25,26} seems reasonable: Watanabe and co-workers proposed a similar face-to-face stacking of an all-aromatic polyester composed of an electron-accepting pyromellitic unit with long side chains.^{26a} Coates and co-workers proposed an analogous solid packing for arylene-vinylene-type oligomers.^{26b} As described above, **1** assumes a linear and coplanar structure (see Figure 1 and Chart 2).

The shift (about 70 nm or ΔE = 3500 cm^{-1} on changing the solution system to the film system; No. 3 in Table 2) observed for PAE-1 is larger than that (approximately 45 nm) observed for a previously reported CT-type copolymer of electron-accepting quinoxaline and electron-donating thiophene.²⁵

In the case of PAE-4 having a stronger electron-accepting unit containing the CN substituent, both its solution and film give the π - π^* absorption band at a

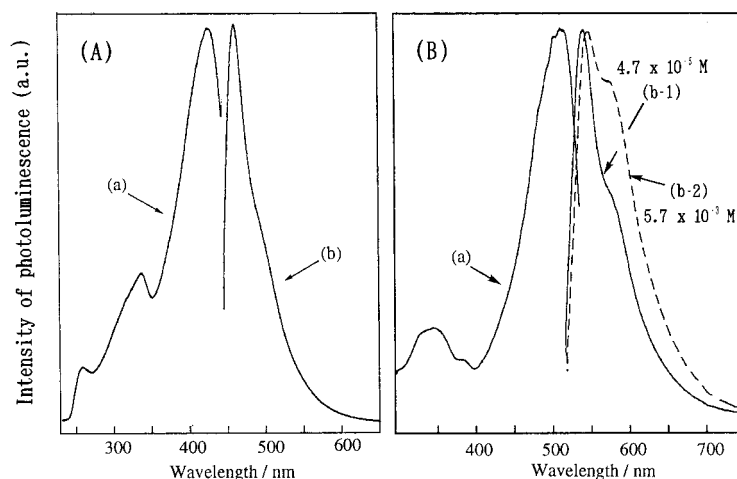
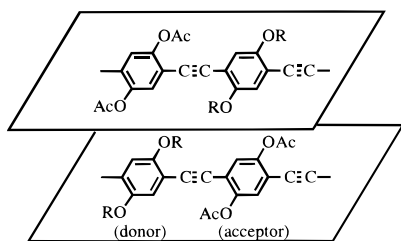


Figure 4. Photoluminescence data of (A) PAE-1 and (B) PAE-4 in chloroform. Lines a and b exhibit the excitation and photoluminescence spectra, respectively. The photoluminescence of PAE-4 was measured at (b-1) lower concentration (4.7×10^{-5} M of the repeating unit) and (b-2) higher concentration (5.7×10^{-3} M of the repeating unit).

Chart 2. A Stacking Model Proposed for CT-Type PAE-1 in Film



considerably longer wavelength region than those of CHCl_3 solutions of PAE-1 (part a in Figure 3) and the usual PAE-type polymers.²¹ This shift to a longer wavelength region may originate from its stronger intermolecular CT structure and its taking a stacked aggregated structure even in solution, similar to the case of head-to-tail-type poly(3-alkylthiophene-2,5-diyl), HT-P3RTh, in poor solvents.^{11f} Such stacking in the solution, however, does not seem to occur for oligomeric products of PAE-4.²⁷ X-ray diffraction data of the polymers suggest a stacked structure and will be described later in this paper. The absorption bands (α) and (β) of PAE-4 (Figure 3b) may originate from single PAE-4 molecule and from the stacked mass composed of PAE-4 molecules, respectively. In this case, the appearance of the absorption band (α) at a longer wavelength than that of the π - π^* absorption band of PAE-1 in CHCl_3 is attributed to an intramolecular, highly charge-transferred structure of PAE-4.

According to the transformation of the OAc group into the OH groups (eq 8), the acceptor unit in PAE-4 (cf. Chart 2) is considered to lose its strong electron-accepting ability, and both the intramolecular and intermolecular CTs seem to be weakened in PAE-5. The absorption peaks of PAE-5, in both solution and film, shift to a shorter wavelength region (part c of Figure 3).

PAE-1-4 give considerably strong photoluminescence with a quantum yield of 25–41% in chloroform (Table 2). As shown in Figure 4, the photoluminescence spectrum exhibits a main peak and a shoulder peak, similar to the photoluminescence spectra of previously reported PAE-type polymers^{7b,c,8,21} and poly(arylenevinylene)-type polymers.²⁸ The data shown in Figure 4 and Table

2 reveal the following features of the photoluminescence of the polymers.

(i) The main photoluminescence peaks of PAE-1 and PAE-4 (Figure 4) seem to appear at the onset positions of the π - π^* absorption band of PAE-1 and the band (α) of PAE-4 (Figure 3b), respectively. The photoluminescence of PAE-1 is considered to originate from single PAE-1 molecule. The photoluminescence data of PAE-4 suggest that the main photoluminescence of PAE-4 is associated with the absorption band (α) that may arise from the single PAE molecule as discussed above.

(ii) The excitation spectrum of PAE-1 (Figure 4A) agree with the absorption spectrum of PAE-1 in chloroform (Figure 3a). On the other hand, the excitation spectrum of PAE-4 (Figure 4B) corresponds to the band (α) of PAE-4, and no peak is observed at the position of the band (β). This feature and feature i suggest that the main photoluminescence is concerned with a photo-process of single PAE molecules and that the photo-excitation of PAE-4 leads to dissociation of the stacked molecules. If this dissociation takes place, emission of light from the stacked mass, which is sometimes observed with stacked π -conjugated polymers,^{11f} will not occur.

(iii) The intensity of the shoulder photoluminescence of PAE-4 increases with increases in the concentration of the polymer, as exhibited in Figure 4B. This result suggests that the photoexcited PAE-4 molecule forms an excimer-like adduct with other PAE-4 molecule(s), especially at the higher concentration of the polymer. Formation of such an excimer-like adduct is sometimes observed with π -conjugated polymers.^{6f} However, the position of the shoulder peak apparently deviates from the onset position of the band (β) of PAE-4, suggesting that the intermolecular interaction in the excimer-like adduct is different from that in the stacked mass of PAE-4 in the ground state.

PAE-5 gives its photoluminescence peak (559 nm) near the onset position of its absorption peak. However, the intensity of the photoluminescence is much weaker than those of the other PAE-type polymers. The excitation spectrum of PAE-5 agrees with the UV-vis absorption spectrum of the polymer.

Electrochemical Response. PPP-2,5-OH in Solution. Part a of Figure 5 exhibits the CV chart of a DMF solution of PPP-2,5-OH under N_2 . The CV chart shows

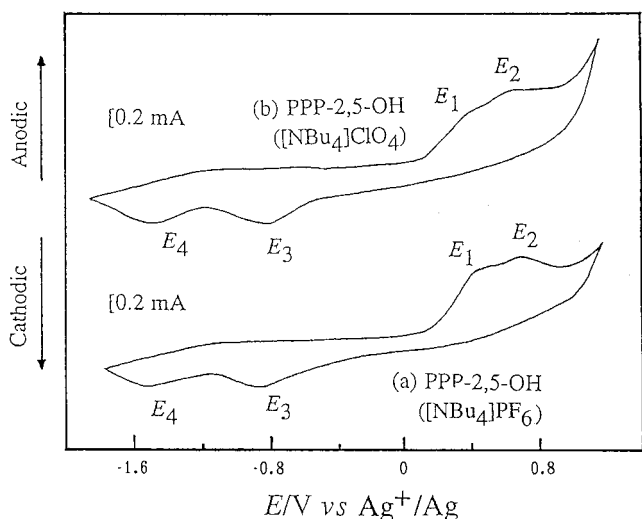
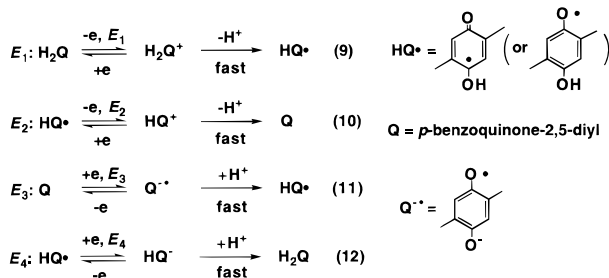


Figure 5. Cyclic voltammograms of (a) PPP-2,5-OH (1.8 mM monomer unit) in a DMF solution of 0.1 M $[\text{NBu}_4]\text{PF}_6$ and (b) PPP-2,5-OH (1.8 mM monomer unit) in a DMF solution of 0.1 M $[\text{NBu}_4]\text{ClO}_4$. Scan velocity = 50 mV s^{-1} , electrode = $1 \times 1 \text{ cm}^2$ Pt plate at room temperature (about 25°C).

Chart 3. Redox Processes in Solution



two oxidation peaks at E_1 and E_2 and two reduction peaks at E_3 and E_4 . The CV data are accounted for by the following electrochemical reactions, including H^+ -transfer, which are based on previous reports on the electrochemical behavior of hydroquinone^{17,29} (see Chart 3). Repeated scanning gave almost the same CV curve (e.g., in the fifth scanning), suggesting that the polymer was stable in the solution and did not undergo complicated reactions.

As depicted in Figure 6, the oxidation peak (e.g., E_2 peak) current is roughly proportional to $v^{1/2}$ (v = sweep velocity), revealing that the diffusion process of PPP-2,5-OH is an important factor in controlling the electric current for the oxidation of PPP-2,5-OH. A similar relationship between the oxidation peak current and $v^{1/2}$ was reported for a PAE-type polymer containing ferrocene units.^{7d}

PPP-2,5-OH in Film. In contrast to the solution system, the CV curve of the PPP-2,5-OH film in a CH_3CN solution strongly depends on the repeating number of scans performed. As shown in parts a and b of Figure 7, the large oxidation peaks at E_1 and E_2 , which are observed at the first scan and correspond to the oxidation of PPP-2,5-OH to PPBQ (poly(*p*-benzoquinone)), become very small in the second scan.

The steep decrease in E_1 and E_2 currents in the second scan is reasonably well accounted¹⁷ for by assuming that (i) the film can release H^+ generated by the oxidation process (eqs 9 and 10) into the solution, whereas (ii) the Q species formed in the film cannot capture H^+ from the solution easily during its reduction processes even

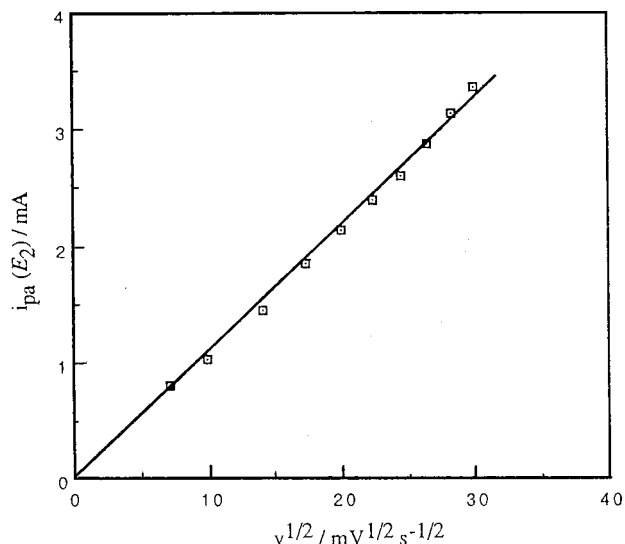


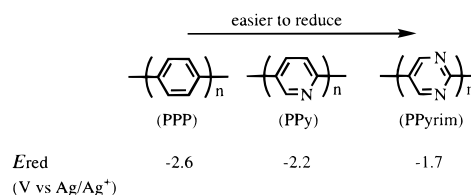
Figure 6. Linear dependence of $i_{\text{pa}}(E_2)$ on $v^{1/2}$ (v = scan velocity) for PPP-2,5-OH (1.8 mM monomer unit) in a DMF solution of 0.1 M $[\text{NBu}_4]\text{PF}_6$. Electrode = $1 \times 1 \text{ cm}^2$ Pt plate.

at the slow scan rate of 20 mV s^{-1} (Figure 7). If the quinone unit Q in the film cannot capture H^+ , the hydroquinone species H_2Q is not regenerated and peaks E_1 and E_2 will become weaker in the second scan.

In the film, the $\text{Q}^{\bullet-}$ (eq 11) and Q^{2-} species formed during the reduction processes at E_3 and E_4 seem to capture NR_4^+ existing at high concentration, instead of H^+ , to give the *n*-doped states^{3b} depicted in Chart 4. Thus, as shown in eq 14, processes E_3 and E_4 in Figure 7 are expressed by the *n*-doping of PPBQ, and peaks E_5 and E_6 are due to *n*-undoping peaks.³⁰ When $[\text{NBu}_4]\text{ClO}_4$ is used, processes E_5 and E_6 seem to overlap (part b of Figure 7).

Although peaks E_1 and E_2 overlap, the total electric charge used for the oxidation (eq 13) can be roughly calculated from the CV chart, and the degree of oxidation of PPBQ is obtained from the total electric charge and the assumed two-electron oxidation. Table 3 gives a summary of the results, which indicate that the oxidation proceeds to a greater degree with a thinner PPP-2,5-OH film and at a slower scan. Employment of LiBF_4 as the electrolyte gives complicated CV results different from those obtained with NBu_4^+ salts (part c of Figure 7), probably due to the known strong interaction of Li^+ with the reduced form of quinones.^{3b,31}

Linear Free-Energy Relationship. The reduction potential E_{red} of π -conjugated poly(arylene)s, Ar_n , normally reflects the electron-accepting properties of the monomeric unit, HArH .^{32b} For example,



The average of E_3 and E_6 in Figure 7 is taken as E_{red} of PPBQ, similar to the case of poly(anthraquinone).^{32b} Figure 8 indicates that plots of E_{red} of PPP, PPy, PPyrim, and PPBQ against EA³² of the corresponding monomeric compound give a linear relationship for

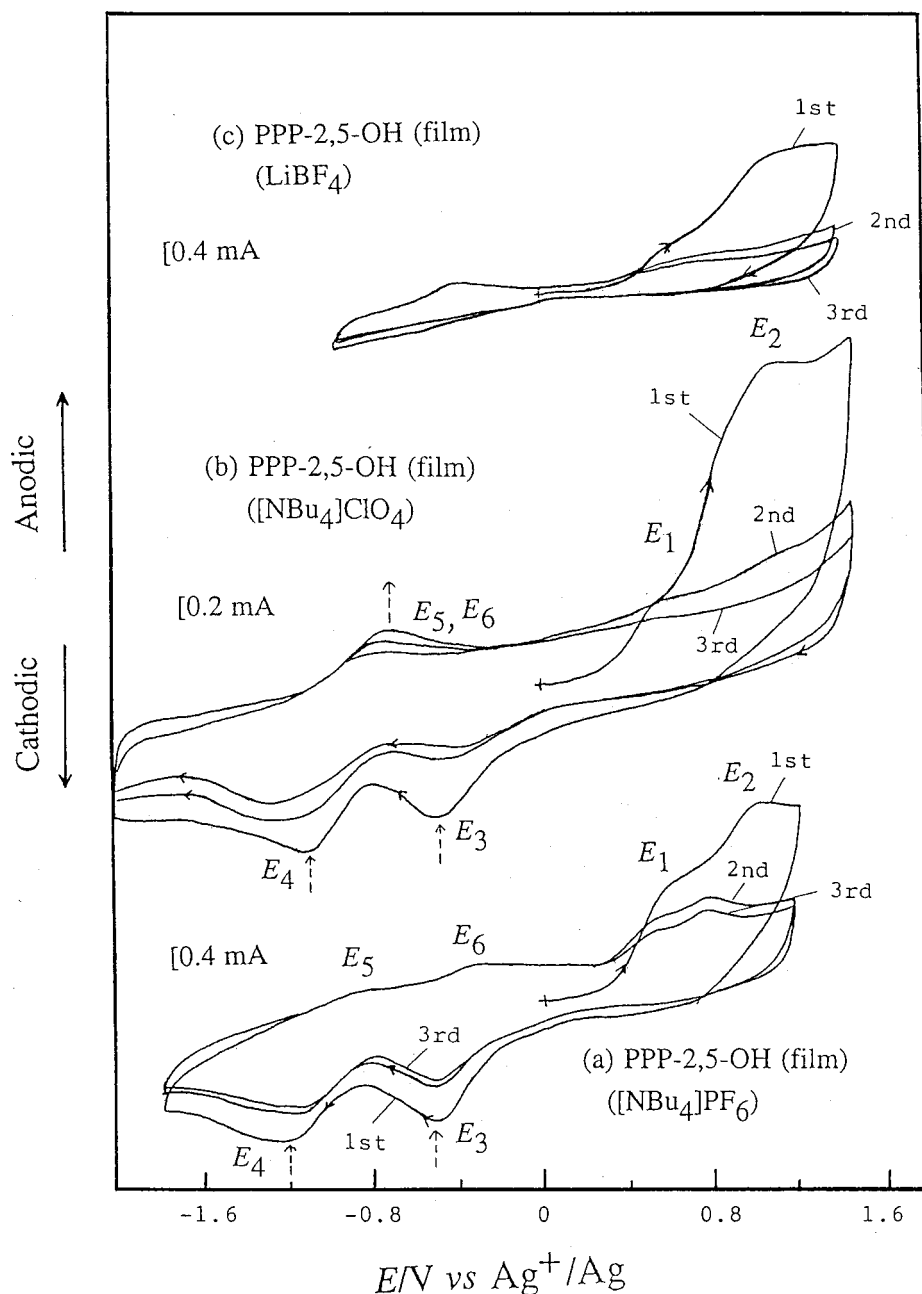
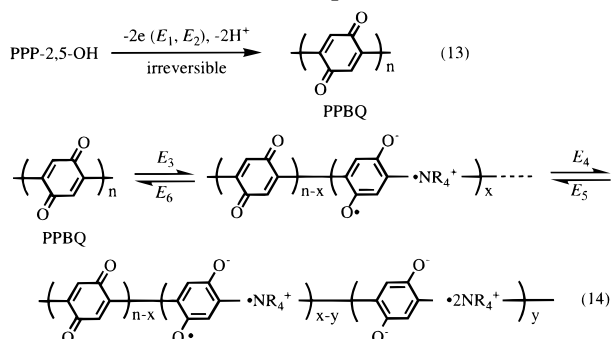


Figure 7. Cyclic voltammograms of the film of PPP-2,5-OH in CH_3CN containing 0.10 M (a) $[\text{NBu}_4]\text{PF}_6$, (b) $[\text{NBu}_4]\text{ClO}_4$, and (c) LiBF_4 . Electrode = $1 \times 1 \text{ cm}^2$ at 20 mV s^{-1} .

Chart 4. Oxidation of PPP-2,5-OH (eq 13) and Redox Processes (*n*-doping and *n*-undoping) of PPBQ in Film (eq 14)



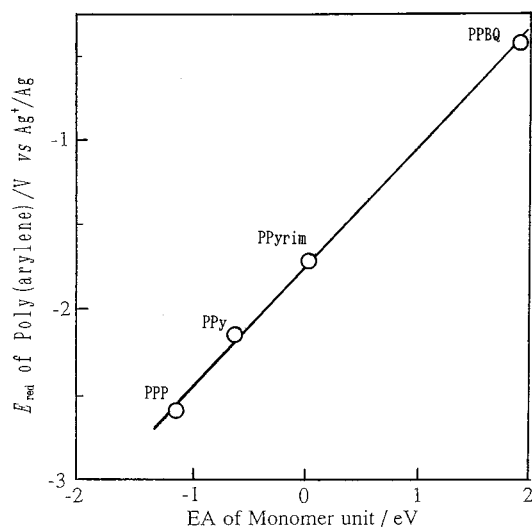
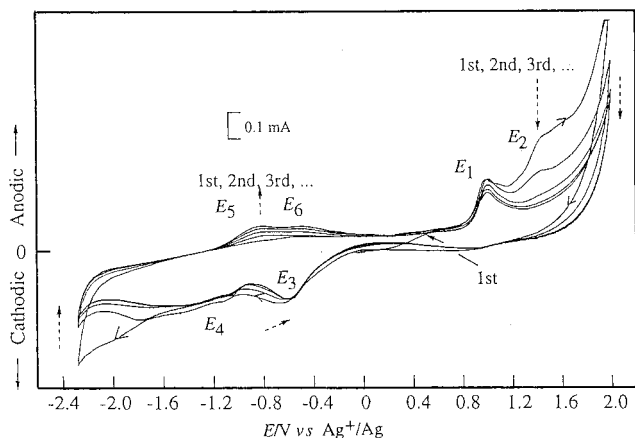
various Ar_n . The slope of this line, $\rho = 0.75$, is comparable to those observed with poly(naphthalene)-type polymers.^{32b}

PAE-5. As depicted in Figure 9, a film of PAE-5 gives rise to a CV chart similar to that of the PPP-2,5-OH film. However, processes E_1 and E_2 take place at higher potentials compared with those observed with PPP-2,5-OH, reflecting the known electron-withdrawing ability of the $-\text{C}\equiv\text{C}-$ ^{7b} and CN groups. The height of the E_2 peak decreases during repeated scanning, and peaks E_5 and E_6 become stronger, similar to the case of the PPP-2,5-OH film. However, in contrast, peak E_1 of the PAE-5 film remains even after repeated scanning, and the CV pattern in the reduction region (the region of peaks E_3 and E_4) varies with the scanning repetition number. Although detailed electrochemical processes have not been revealed, these results suggest that H^+ can partly move into the PAE-5 film and the reduced quinone, Q^{2-} , can, at least partly, capture H^+ . Movement of H^+ through organic media is considered to be an important process in living systems and has attracted the attention

Table 3. Degree of Oxidation of PPP-2,5-OH to PPBQ at Various Thicknesses of the PPP-2,5-OH Film and Sweep Rates^a

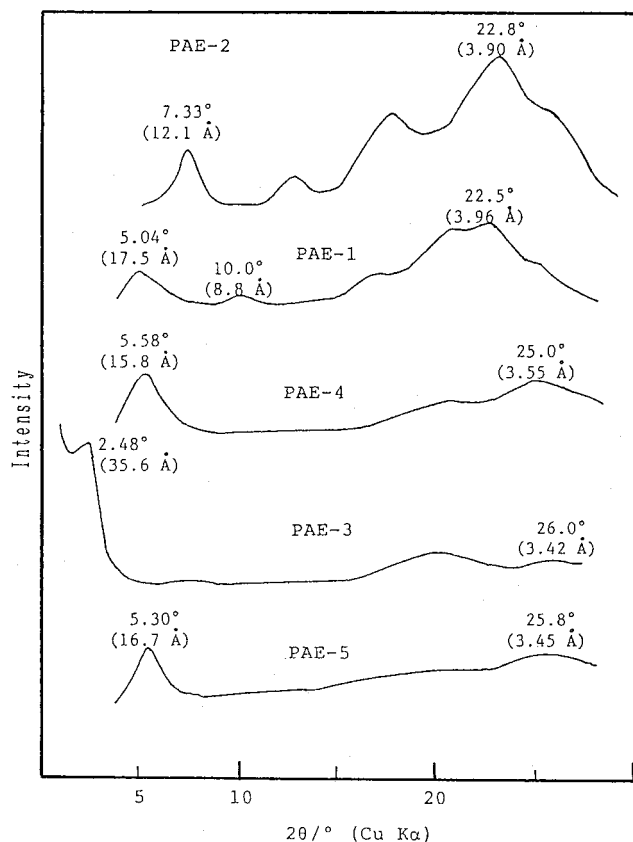
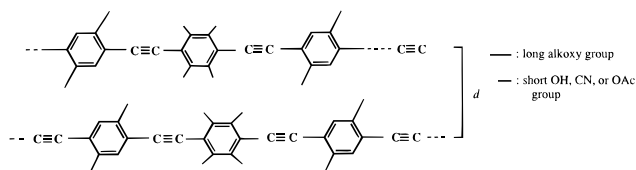
thickness ^b (10 ⁻⁷ mol cm ⁻²)	sweep rate (mV s ⁻¹)	degree of oxidation (%)
0.925	30	96
0.925	50	83
0.925	70	83
0.925	90	59
1.85	30	58
1.85	50	54
1.85	90	57
2.76	30	55
2.76	90	57
3.70	30	55
3.70	70	42
3.70	90	33

^a In a CH₃CN solution of [NBu₄]PF₆ (0.10 M). ^b Thickness of the film is given in mole of the monomeric unit of PPP-2,5-OH on a 1 × 1 cm² Pt electrode.

**Figure 8.** Plots of E_{red} of $(-\text{Ar})_n$ vs EA of HArH. A linear correlation with a slope of 0.75 is obtained.**Figure 9.** CV chart of a film of PAE-5 laid on a Pt plate (1 × 1 cm²) in a CH₃CN solution of [NBu₄]BF₄ at 20 mV s⁻¹.

of biochemists.³³ Recently, quinone-assisted transport of H⁺ and production of ATP in an artificial membrane have been reported.^{33a} Oxidation of PAE-5 with NO₂ in DMF gave a dark brown product whose IR spectrum showed a strong peak at 1720 cm⁻¹, which indicated transformation of the hydroquinone unit of PAE-5 into a *p*-quinone unit.

XRD Data of PAE-Type Polymers. Molecular assembly of organic and inorganic molecules is a subject

**Figure 10.** Powder X-ray diffraction patterns of PAE-type polymers. The peak of PAE-1 at $d = 8.8$ Å may be assigned to the second peak of $d = 17.5$ Å.**Chart 5. Distance between the Core Main Chains in the Postulated Solid Structure**

of recent interest.³⁴ Aromatic polymers with long side chains often assume a face-to-face stacked structure^{26a} assisted by side-chain crystallinity.³⁵ Preparation of π -conjugated poly(arylene)s with side chains^{5c,11f,23-25} and their stacking properties have also attracted the attention of chemists. Figure 10 shows X-ray diffraction patterns of PAE-type polymers having long side chains. All of these polymers give clear X-ray diffraction peaks, indicating that they form certain ordered structures in the solid state. If the polymer takes a linear and coplanar structure similar to that of **1**, a peak in the low-angle region from about $2\theta = 2.5$ to 7.5° may be assigned to the distance between the core polymer chains separated by the long OR chain, which is similar to cases of aromatic polymers with such long side chains.^{11f,23,24,26,34}

In this case (see Chart 5), the data exhibited in Figure 10 and additional experimental data reveal the following features of PAE-type polymers.

(1) The postulated core-to-core distance estimated from the position of the peak at the low angle is determined not only by the length of the OR group but also by the presence or absence of the CN group. The polymers with the CN group (PAE-3 and PAE-4) have a longer core-to-core distance than the corresponding

polymers without the CN group.

(2) PAE-5 gives a diffraction pattern analogous to that of PAE-4, revealing that the packing mode of PAE-4 is maintained even after transformation of the OAc group into the OH group. The OAc and OH groups in PAE-4 and PAE-5, respectively, are considered not to disturb the coplanar π -conjugated structure of the main chain, and the basic packing style of PAE-4 seems to be maintained even after the chemical change of the OAc group to the OH group.

(3) The PAE-type polymers (PAE-1–4) prepared at low temperature or at short reaction times (and consequently having a lower molecular weight)²⁷ do not give sharp X-ray diffraction peaks. The PAE-type polymers with the low molecular weights do not show the bathochromic shift in the solid state (vide ante).²⁷ These results support the belief that the bathochromic shift in the solid state is caused by the CT interaction between the ordered polymer molecules with a sufficient chain length (cf. Chart 2).

Conclusion and Scope

Poly(hydroquinone)s have been prepared by organo-metallic polycondensation. PPP-2,5-OH can be electrochemically oxidized to poly(*p*-benzoquinone). The electrochemical reduction behavior of poly(*p*-benzoquinone) depends strongly on the physical state of the polymer. In the solution, the polymer undergoes the usual reduction to PPP-2,5-OH, whereas its reduction in the solid state is understood in terms of *n*-doping. Because of the presence of an expanded π -conjugation system, the UV-vis spectra of the polymers show bathochromic shifts of the π - π^* absorption band from the peak positions of their corresponding monomeric compounds. In the solid state, an additional shift to a longer wavelength region is observed with the PAE-type polymers, presumably due to an intermolecular CT interaction. The polymers may be useful in preparing new polymer-modified electrodes and electric devices^{1,36,37} that require electron-accepting and electron-carrying organic layers.

Experimental Section

Materials. Ni(cod)₂,^{38a} Pd(PPh₃)₄,^{38b} 1,4-dibromo-2,5-hydroxybenzene,³⁹ 1,4-dimethoxy-2,5-dicyanobenzene,⁴⁰ and 1,4-dialkoxy-2,5-diethynylbenzene ($R = n\text{-C}_{12}\text{H}_{25}$) (monomer c)^{21b} were prepared according to the literature. Commercially available anhydrous acetonitrile and DMF were stored under dry argon or nitrogen and used for CV. Salts for the CV measurement were dried under vacuum.

Synthesis. *1,4-Dibromo-2,5-diacetoxybenzene (monomer a; R¹ = R² = H).* Monomer a was prepared by reaction of 1,4-dibromo-2,5-hydroxybenzene with acetic anhydride in the presence of a drop of perchloric acid. Yield: 44%. Anal. Found: C, 34.1; H, 2.3; Br, 45.45. Calcd for C₁₀H₈Br₂O₄: C, 34.2; H, 2.4; Br, 45.1%. IR(KBr, cm⁻¹): 1750, 1060. ¹H NMR (CDCl₃): δ 7.40 (s, 2H), 2.35 (s, 6H). ¹³C NMR(CDCl₃): δ 167.6, 146.1, 127.4, 114.9, 20.3. Monomer a with R¹ = H and R² = *n*-C₆H₁₃ was prepared analogously in 38% yield. ¹H NMR (CDCl₃): δ 7.28 (s, 1H), 2.69 (t, 2H), 2.37 (s, 3H), 2.35 (s, 3H), 1.31–1.55 (m, 8H), 0.90 (t, 3H). This compound was also prepared by Kallitsis and co-workers recently via a different route.⁴¹

1,4-Dibromo-2,5-diacetoxy-3,6-dicyanobenzene (monomer b; R¹ = R² = CN). 1,4-Dimethoxy-2,5-dicyanobenzene⁴⁰ (5.50 g, 29.5 mmol), AlCl₃ (27.5 g, 206 mmol), and NaCl (5.50 g, 94.0 mmol) were ground in an agate mortar under Ar. The mixture was heated at 180–200 °C for 1 h under Ar. After extra AlCl₃ was quenched by distilled water, crude 1,4-dihydroxy-2,5-dicyanobenzene was extracted with diethyl ether and dried with MgSO₄. Diethyl ether was removed by evaporation, and

the crude product was recrystallized from water. Yield: 49%. IR(KBr): 3248, 2292. ¹H NMR (DMSO-*d*₆): δ 11.04 (s, 2H, OH), 7.20 (s, 2H).

To 1,4-dihydroxy-2,5-dicyanobenzene thus prepared (0.40 g, 2.5 mmol) were added glacial acetic acid (5 mL) and Br₂ (1.20 g, 7.5 mmol) slowly, and the reaction mixture was stirred for 2 h under reflux. The yellow precipitate was separated by filtration and recrystallized from a mixture of ethanol and H₂O (3:7) to obtain 1,4-dibromo-2,5-dihydroxy-3,6-dicyanobenzene in 71% yield. Anal. Found: C, 30.5; H, 0.6; N, 8.8; Br, 49.9%. Calcd: C, 30.2; H, 0.6; N, 8.8; Br, 50.3%. IR(KBr): 3296, 2244. ¹H NMR (acetone-*d*₆): δ 9.97 (s, 2H, OH). ¹³C NMR (acetone-*d*₆): δ 152.3, 114.7, 114.3, 111.2.

To 1,4-dibromo-2,5-dihydroxy-3,6-dicyanobenzene thus obtained (1.0 g, 6.29 mmol) was added 30 mL of glacial acetic acid slowly. After addition of a drop of perchloric acid, the mixture was stirred for 48 h at room temperature. The reaction mixture was poured into 300 g of ice-water, and the product was extracted with 200 mL of chloroform. The extract was washed with an aqueous solution of Na₂CO₃ thoroughly and dried with MgSO₄. The solution was condensed to obtain a white solid, which was recrystallized from ethyl acetate to obtain white needles of monomer b (R¹ = R² = CN). Anal. Found: 36.3; H, 1.6; N, 7.1; Br, 39.5%. Calcd: C, 35.9; H, 1.5; N, 7.0; Br, 39.8%. IR(KBr): 2244, 1790. ¹H NMR (CDCl₃): δ 2.53 (s). ¹³C NMR (DMSO-*d*₆): δ 167.2, 149.4, 120.9, 116.8, 112.3, 20.0.

Monomer c. Monomer c with R = *n*-C₆H₁₃ was prepared in a manner similar to that reported in the literature.^{21b} Anal. Found: C, 49.4; H, 6.6; Br, 36.4%. Calcd: C, 49.6; H, 6.5; Br, 36.6%. X-ray crystallographic data: monoclinic; *a* = 9.460 (4), *b* = 6.773 (2), and *c* = 15.739 (5) Å; β = 91.06 (3)°; space group = *P*2₁/*n* (no. 14); *D*_{calc} = 1.075 g cm⁻³; *R* = 0.051; *R*_w = 0.044.

Model Compound 1 (eq 5). To a mixture of 1,4-dibromo-2,5-diacetoxybenzene (monomer b; R¹ = R² = H) (0.50 g, 1.4 mmol), Pd(PPh₃)₄ (82 mg, 0.071 mmol), CuI (14 mg, 0.071 mmol), toluene (3 mL), and NEt₃ (3 mL) was added 4-ethynyltoluene (363 mg, 3.13 mmol) slowly, and the mixture was stirred for 6 h at 60 °C. The reaction mixture was poured into excess methanol to obtain a white precipitate, which was purified by column chromatography on SiO₂ (eluent = 1:1 mixture of CH₃COOC₂H₅ and toluene). Yield: 61%. Anal. Found: C, 79.4; H, 5.3%. Calcd: C, 79.6; H, 5.3%. IR(KBr): 2216, 1758. ¹H NMR (CDCl₃): δ 7.35–7.14 (m, 8H), 2.35 (12 H). The molecular structure as determined by X-ray crystallography is given in Figure 1.

Model Compound 2. **2** was also prepared in 57% yield, and its IR (2236, 2208, and 1778 cm⁻¹) and ¹H NMR ((CDCl₃): δ 7.87–7.16 (m, 8H), 2.50–2.40 (6H)) agreed. However, repeated recrystallizing of **2** from methylene chloride led to partial hydrolysis of the OAc group, and obtaining a crystal suited for the X-ray crystallography was not possible.

Preparation of Polymers. *PPP-2,5-OAc.* A mixture of Ni(cod)₂ (3.13 g, 11.4 mmol), cod (1.23 g, 11.4 mmol), bpy (1.77 g, 11.4 mmol), and 1,4-dibromo-2,5-diacetoxybenzene (2.0 g, 5.7 mmol) in 50 mL of DMF was stirred under N₂ for 48 h at 60 °C. The reaction mixture was condensed to 10 mL and poured into dilute hydrochloric acid. The cream precipitate was washed with dilute hydrochloric acid (twice), an aqueous solution of disodium ethylenediaminetetraacetate (twice), dilute hydrochloric acid (once) in this order and dried under vacuum. Yield: 72%. Anal. Found: C, 61.5; H, 4.5; Br, 0%. Calcd for C₁₀H₈O₄: C, 62.5; H, 4.2%. Calcd for C₁₀H₈O₄·0.1H₂O: C, 61.9; H, 4.3%. IR(KBr): 2932, 1762, 1207. ¹H NMR (DMF-*d*₇): δ 6.9–7.6 (m, 2H), 2.0–2.6 (m, 6H).

PPP-2,5-OH. A mixture of PPP-2,5-OAc (0.30 g, 1.6 mmol monomer unit) and LiAlH₄ (0.25 g, 6.5 mmol) in 50 mL of THF was stirred for 48 h at 40 °C. After removal of THF by evaporation, the residue was washed with dilute hydrochloric acid repeatedly to obtain a black solid of PPP-2,5-OH in 100% yield. Anal. Found: C, 57.2; H, 5.2%. Calcd for (C₆H₄O₂·H₂O)_{*n*}: C, 57.1; H, 4.8%. ¹H NMR (DMF-*d*₇; under N₂): δ 6.8–7.6 (m, 2H, aromatic-H), 8.8–9.7 (m, 2H, OH) at 25 °C. At 100 °C, the OH signal was shifted to δ 8.1–9.2 (peak = δ 8.4) and broadened, whereas the peak position of the aromatic-H

was essentially unvaried at 100 °C. ^1H NMR spectrum of hydroquinone in DMF- d_7 showed similar temperature dependence, at 25 °C: δ 6.67 (s, 4H, aromatic-H), 8.76 (s, 2H, OH). At 50 °C: δ 6.61, 8.58. At 100 °C: δ 6.65, 8.19.

PAE-Type Polymers. The polymerization was carried out under N_2 in a manner analogous to those previously reported.^{7,8,21} PAE-1 was prepared by using 1,4-dibromo-2,5-diethoxybenzene (200 mg, 0.57 mmol), 1,4-didodecyloxy-2,5-diethynylbenzene (280 mg, 0.57 mmol), $\text{Pd}(\text{PPh}_3)_4$ (33 mg, 0.028 mmol), and CuI (5.4 mg, 0.028 mmol) in a 1:1 mixture of toluene and NEt_3 at 60 °C for 24 h, and worked-up was done in a manner similar to that previously reported.⁷ Yields and molecular weights are given in Table 1. Anal. Found: C, 74.3; H, 8.6; Br, 3.7%. Calcd for $\text{Br}(\text{C}_{44}\text{H}_{60}\text{O}_6)_6\text{C}_{10}\text{H}_8\text{O}_2\text{Br}$: C, 74.3; H, 8.4; Br, 3.6%. PAE-2–4 were prepared analogously. PAE-4: Anal. Found: C, 69.8; H, 6.1; N, 4.8; Br, 2.8%. Calcd for $\text{Br}(\text{C}_{34}\text{H}_{34}\text{N}_2\text{O}_6)_{10}\text{C}_{12}\text{H}_6\text{N}_2\text{O}_4\text{Br}$: C, 69.9; H, 5.8; N, 5.1; Br, 2.6%. PAE-5 was prepared by a reaction of PAE-4 with KOH in a 1:2:2 mixture of $\text{H}_2\text{O}/\text{DMF}/\text{THF}$ at 50 °C for 40 h. The product was neutralized with dilute hydrochloric acid and dried. Its IR spectrum (see Supporting Information) revealed complete hydrolysis of OAc.

Measurements. Electrochemical and optical data as well as other analytical data were obtained in manners similar to those previously reported.^{5,7} The quantum yield of the photoluminescence was calculated by using a diluted sulfuric acid (0.50 M) solution of quinine. The polymer films for the CV measurements were obtained by casting solutions of the polymers. The CV charts were recorded by using a Hokuto Denko HA-501 galvanostat/potentiostat and a Hokuto Denko KB-104 function generator or a Hokuto Denko HABF501 Potential/FG set. Light scattering analysis was carried out with an Otsuka Electronics DLS-700 dynamic light scattering spectrophotometer.

X-ray Diffraction Analysis of 1. Crystal data: $\text{C}_{28}\text{H}_{22}\text{O}_4$, $M_r = 422.48$; monoclinic; $P2_1/n$ (No. 14); $a = 12.867$ (7), $b = 5.785$ (6), and $c = 16.678$ (8) Å; $\beta = 111.15$ (4)°; $V = 1157$ (1) Å³; $Z = 2$; $\mu = 0.80$ cm⁻¹; $F(000) = 444$; $D_{\text{calc}} = 1.212$ Mg m⁻³; 2θ range = 6.0–50.0°; hkl ranges: $0 \leq h \leq 13$; $-16 \leq k \leq 6$; $0 \leq l \leq 18$; no. of unique reflections = 1972; no. of used reflections ($I > 3\sigma(I)$) = 413; no. of variables = 145. The final $R(F_o)$ and $R_w(F_o)$ values were 0.045 and 0.044, respectively; $R = \sum ||F_o| - |F_c|| / \sum |F_o|$; $R_w = \sum w|F_o - F_c|^2 / \sum w|F_o|^2$ ^{1/2}; weighting scheme $w = \{[\sigma(F_o)]^2\}^{-1}$. The unit cell parameters were obtained by least-squares refinement of 2θ value of 15 reflections with $6.8^\circ \leq 2\theta \leq 12.4^\circ$.

Intensities were collected on a Rigaku AFC-5R automated four-cycle diffractometer by using graphite-monochromated Mo K α radiation ($\lambda = 0.71069$ Å) and the ω - 2θ method. Empirical absorption correction (ψ -scan method) of the collected data was applied. Calculations were carried out by using the program package teXsan on a VSX-II computer. Atomic scattering factors were taken from the literature.⁴² A full-matrix least-squares refinement was used for non-hydrogen atoms with anisotropic thermal parameters. Hydrogen atoms were located by assuming ideal positions and were included in the structure calculation with further refinement of the parameters.

Acknowledgment. We are grateful to Drs. Y. Hayashi, I. Yamaguchi, J. C. Choi, and Y. Muramatsu of our laboratory for experimental support.

Supporting Information Available: IR, UV, and NMR data, and CV data. This material is available free of charge via the Internet at <http://pubs.acs.org>.

References and Notes

- (1) (a) Nalwa, H. S., Ed. *Handbook of Organic Conductive Molecules and Polymers*, Vol. 2; John Wiley: New York, 1997. (b) Kuzmany, H.; Mehring, M.; Roth, S., Ed. *Electronic Properties of Polymers*; Springer: Berlin, 1992. (c) Skotheim, T. A., Ed. *Handbook of Conducting Polymers*; Marcel Dekker: New York, 1986; Vols. I and II.
- (2) (a) Skancke, A.; Skancke, P. N. *Chem. Quinoid Compd.* **1988**, 2, 1. (b) Evans, D. H. In *Encyclopedia of Electrochemistry of Elements*; Bard, A. J.; Lund, H.; Eds.; Marcel Dekker: New York, 1978; Vol. XII, p 1. (c) Doron, A.; Portnoy, M.; Lion-Dagan, M.; Katz, E.; Willner, I. *J. Am. Chem. Soc.* **1996**, 118, 8937. (d) Lei, Y.; Anson, F. C. *J. Am. Chem. Soc.* **1995**, 117, 9849. (e) Arai, G.; Takahashi, S.; Yasumori, I. *J. Electroanal. Chem.* **1996**, 410, 173. (f) Granath, H. E. M.; Schultz, G. *Acta Chem. Scand.* **1954**, 8, 1442.
- (3) (a) Wang, P.; Martin, B. D.; Parida, S.; Rethwisch, D. G.; Dordick, J. S. *J. Am. Chem. Soc.* **1995**, 117, 12885. (b) Yamamoto, T.; Etori, H. *Macromolecules* **1995**, 28, 3371. (c) Etori, H.; Kanbara, T.; Yamamoto, T. *Chem. Lett.* **1994**, 461. (d) Yamamoto, T.; Matsuzaki, T.; Minetomo, A.; Kawazu, Y.; Ohashi, O. *Bull. Chem. Soc. Jpn.* **1996**, 69, 3461. (e) Muramatsu, Y.; Yamamoto, T. *Chem. Lett.* **1997**, 581.
- (4) Yamamoto, K.; Asada, T.; Nishide, H.; Tsuchida, E. *Bull. Chem. Soc. Jpn.* **1990**, 63, 1211.
- (5) (a) Yamamoto, T.; Ito, T.; Kubota, K. *Chem. Lett.* **1988**, 153. (b) Yamamoto, T.; In *Handbook of Organic Conductive Molecules and Polymers*; Vol. 2 Nalwa, H. S., Ed.; John Wiley: Chichester, 1997; p 171. (c) Yamamoto, T. *Bull. Chem. Soc. Jpn.* **1999**, 72, 621.
- (6) (a) Wang, Y.; Quirk, R. P. *Macromolecules* **1995**, 28, 3495. (b) Kreyenschmidt, M.; Uckert, F.; Müllen, K. *Macromolecules* **1995**, 28, 4577. (c) Ueda, M.; Seino, Y.; Haneda, Y.; Yoneda, M.; Sugiyama, J. *J. Polym. Sci., Part A, Polym. Chem.* **1994**, 32, 675. (d) Yamamoto, T.; Suganuma, H.; Maruyama, T.; Kubota, K. *J. Chem. Soc., Chem. Commun.* **1995**, 1613. (e) Nanos, J. I.; Kampf, J. W.; Curtis, M. D.; Gonzalez, L.; Martin, D. C. *Chem. Mater.* **1995**, 7, 2332. (f) Yamamoto, T.; Maruyama, T.; Zhou, Z.-H.; Ito, T.; Fukuda, T.; Yoneda, U.; Begum, F.; Ikeda, T.; Sasaki, S.; Takezoe, H.; Fukuda, A.; Kubota, K. *J. Am. Chem. Soc.* **1994**, 116, 4832. Recently, polypyridine with a M_w of 6300 has also been prepared.
- (7) (a) Sanechika, K.; Yamamoto, T.; Yamamoto, A. *Bull. Chem. Soc. Jpn.* **1984**, 57, 753; *Polym. Prepr.* **1981**, 30, 160. (b) Yamamoto, T.; Yamada, W.; Takagi, M.; Kizu, K.; Maruyama, T.; Ooba, N.; Tomaru, S.; Kaino, T.; Kubota, K. *Macromolecules* **1994**, 27, 6620. (c) Yamamoto, T.; Honda, K.; Ooba, N.; Tomaru, S. *Macromolecules* **1998**, 31, 7. (d) Yamamoto, T.; Morikita, T.; Maruyama, T.; Kubota, K.; Katada, M. *Macromolecules* **1997**, 30, 5390.
- (8) (a) Trumbo, D. L.; Marvel, C. S. *J. Polym. Sci., Part A: Polym. Chem.* **1986**, 24, 2311. (b) Wautelet, P.; Moroni, M.; Moigne, J. L.; Pham, A.; Bigot, J.-Y. *Macromolecules* **1996**, 29, 446. (c) Li, J.; Pang, Y. *Macromolecules* **1997**, 30, 7487. (d) Mangel, T.; Eberhardt, A.; Scherf, U.; Bunz, U. H. F.; Müllen, K. *Makromol. Rapid Commun.* **1995**, 16, 571.
- (9) (a) Fox, M. A.; Dulay, M. T.; Krosley, K. *J. Am. Chem. Soc.* **1994**, 116, 10992. (b) Xu, X.-H.; Bard, A. J. *J. Am. Chem. Soc.* **1995**, 117, 2627. (c) Steiger, A.; Anson, F. C. *Inorg. Chem.* **1996**, 36, 4138. (d) Debad, J. D.; Bard, A. J. *J. Am. Chem. Soc.* **1998**, 120, 2476. (e) Debad, J. D.; Morris, J. C.; Lynch, V.; Magnus, P.; Bard, A. J. *J. Am. Chem. Soc.* **1996**, 118, 2374. (f) Anson, F. C.; Blauch, D. N.; Saveant, J.-M.; Shu, C. F. *J. Am. Chem. Soc.* **1991**, 113, 1922. (g) Bhugun, I.; Anson, F. C. *J. Electroanal. Chem.* **1997**, 430, 155. (h) Fabre, B.; Bidan, G. *J. Chem. Soc., Faraday Trans.* **1997**, 93, 591.
- (10) (a) Hoang, P. M.; Holdcroft, S.; Funt, B. L. *J. Electrochem. Soc.* **1985**, 132, 2129. (b) Funt, B. L.; Hoang, P. M. *J. Electroanal. Chem.* **1983**, 154, 229. (c) Day, R. W.; Inzel, G.; Kinstle, J. F.; Chambers, J. Q. *J. Am. Chem. Soc.* **1982**, 104, 6804. (d) Inzelt, G.; Chambers, J. Q.; Kinstle, J. F.; Day, R. W. *J. Am. Chem. Soc.* **1984**, 106, 3396.
- (11) (a) Chen, T.-A.; Wu, X.; Rieke, R. D. *J. Am. Chem. Soc.* **1995**, 117, 233. (b) McCullough, R. D.; Tristram-Nagle, S.; Williams, S. P.; Lowe, R. D.; Jayaraman, M. *J. Am. Chem. Soc.* **1993**, 115, 4910. (c) Miyazaki, Y.; Yamamoto, T. *Synth. Met.* **1944**, 64, 69. (d) Yamamoto, T.; Sanechika, K. *Chem. Ind. (London)* **1982**, 301. (e) Yamamoto, T.; Sanechika, K.; Yamamoto, A. *Bull. Chem. Soc. Jpn.* **1983**, 56, 1497; U.S. Patent 1985-4521589. (f) Yamamoto, T.; Komarudin, D.; Arai, M.; Lee, L.-B.; Suganuma, H.; Asakawa, N.; Inoue, Y.; Kubota, K.; Sasaki, S.; Fukuda, T.; Matsuda, H. *J. Am. Chem. Soc.* **1998**, 120, 2047.
- (12) (a) Yamamoto, T.; Suganuma, H.; Maruyama, T.; Inoue, T.; Muramatsu, Y.; Arai, M.; Komarudin, D.; Ooba, N.; Tomaru, S.; Sasaki, S.; Kubota, K. *Chem. Mater.* **1997**, 9, 1217. (b) Yamamoto, T.; Sugiyama, K.; Kushida, T.; Inoue, T.; Kanbara, T. *J. Am. Chem. Soc.* **1996**, 118, 3930.
- (13) (a) Yamamoto, T.; Ishizu, J.; Kohara, T.; Komiya, S.; Yamamoto, A. *J. Am. Chem. Soc.* **1980**, 102, 3758. (b) Bauld, N. L.

- Tetrahedron Lett.* **1962**, 859. (c) Grab, M. G.; Fering, A. E.; Auman, B. C.; Percec, V.; Zhao, M.; Hill, D. H. *Macromolecules* **1996**, *29*, 7284.
- (14) The ^1H NMR spectra of PPP-2,5-OAc and PPP-2,5-OH give multiplet peaks for aromatic H, OAc, and OH protons, suggesting the presence of rotamers. The CPK molecular models of $\text{H}-\text{C}_6\text{H}_2(\text{OY})_2-\text{C}_6\text{H}_2(\text{OY})_2-\text{C}_6\text{H}_2(\text{OY})_2\text{H}$ ($\text{Y} = \text{H}$ or Ac) as a trimeric model of the polymer suggest a large energy barrier for the free rotation. If all of the benzene rings are arranged perpendicularly to each other, there apparently exist two isomers (trans and cis) in view of the positions of the two $o\text{-OY}$ groups in the both end phenyl groups of the trimeric model compound. Even when the dihedral angle deviates from 90° , there exist similar cis-oid and trans-oid isomers concerning the two $o\text{-OY}$ groups if the free rotation is hindered. The presence of such rotamers (or microstructures) will give various kinds of the aromatic, OAc, and OH protons in the polymers. For PPP-2,5-OH, the OH signals are broadened at elevated temperature presumably due to an exchange reaction on the NMR time scale (cf. the Experimental Section).
- (15) (a) Glaser, C. *Chem. Ber.* **1869**, *2*, 422. (b) *The Merck Index*, 9th Ed.; Merck: Rahway, N. J., 1973; p. ONR-36.
- (16) (a) Nicholls, D. *Pergamon Texts in Inorganic Chemistry*, Vol. 24; Pergamon Press: Oxford, 1973; p. 1142. (b) Feigl, F.; Anger, V. *Spot Tests in Inorganic Analysis*; Elsevier: Amsterdam, 1972; p. 328. (c) Yamamoto, T.; Takeuchi, M., unpublished results. (d) The refractive index increment ($\Delta n/\Delta c$) for the DMF-PPP-2,5-OH system was 0.80 mL g^{-1} at 21°C .
- (17) Yamamoto, T.; Kimura, T. *Macromolecules* **1998**, *31*, 2683.
- (18) (a) Issa, R. M.; Sadek, H.; Ezzat, I. I. *Z. Phys. Chem. Neue Folge* **1971**, *74*, 17. (b) Santary, F.; Waltrvá, D.; Hruban, L. *Coll. Czechoslov. Chem. Commun.* **1972**, *37*, 1825. (c) Ranjith, S. K. A.; Umapathy, S.; McQuillan, A. J. *J. Electroanal. Chem.* **1990**, *284*, 229. (d) Ewast, R. C., Ed. *CRC Handbook of Chemistry and Physics*, 58th ed.; CRC Press: Cleveland, 1977. (e) The absorption peak of PPP-2,5-OAc appears at a considerably longer wavelength than that of an acetate of *p*-tetrahydroquinone ($\lambda_{\text{max}} = 290 \text{ nm}$; Erdtman, H.; Granath, M.; Schultz, G. *Acta Chim. Scand.* **1954**, *8*, 1442).
- (19) (a) Addition of NaOH first leads to appearance of a new $\pi-\pi^*$ absorption peak at 382 nm , which seems assignable to singly anionized PPP-2,5-OH, $[\text{C}_6\text{H}_2(\text{OH})\text{O}^-]_n$. The $\pi-\pi^*$ absorption peak is finally shifted to 415 nm (cf. Figure 1 and Supporting Information; assigned to $[\text{C}_6\text{H}_2(\text{O}^-)_2]_n$) by addition of excess NaOH. The $\pi-\pi^*$ absorption peak reverts to the original position (345 nm) of PPP-2,5-OH on addition of excess HCl. The $\text{p}K_{\text{a}}$ (1) and $\text{p}K_{\text{a}}$ (2) values for the first and second dissociation were roughly estimated at 11 and 11.7, respectively, from the change of the spectrum. (b) Yilmaz, M.; Beligöz, H. *Energy Sources* **1991**, *13*, 211.
- (20) (a) Yamamoto, T.; Lee, B.-L. *Chem. Lett.* **1996**, 65. (b) Yamamoto, T.; Lee, B.-L.; Saitoh, Y.; Inoue, T. *Chem. Lett.* **1996**, 679.
- (21) (a) Yamamoto, T.; Takagi, M.; Kizu, K.; Maruyama, T.; Kubota, K.; Kanbara, H.; Kurihara, T.; Kaino, T. *J. Chem. Soc., Chem. Commun.* **1993**, 797. (b) Moroni, M.; Moigne, J. L.; Luzzati, S. *Macromolecules* **1994**, *27*, 7, 562. The PAE-type polymers usually show the $\pi-\pi^*$ absorption peaks in a range of $380\text{--}440 \text{ nm}$ in solutions.
- (22) Splitting of the peak in the film may originate from vibronic interaction; the splitting (ca. 1400 cm^{-1}) roughly agrees with the frequency of the ring vibration of the aromatic unit. Similar splitting of the absorption peak has been reported for films of regioregular poly(3-alkylthiophene)s.^{23–25}
- (23) (a) McCullough, R. D.; Tristram-Nagle, S.; Williams, S. P.; Lowe, R. D.; Jayaraman, M. *J. Am. Chem. Soc.* **1993**, *115*, 4910. (b) McCullough, R. D.; Ewband, P. C.; Lowewe, R. S. *J. Am. Chem. Soc.* **1997**, *119*, 633.
- (24) Chen, T.-A.; Wu, X.; Rieke, R. D. *J. Am. Chem. Soc.* **1995**, *117*, 233.
- (25) Yamamoto, T.; Zhou, Z.-H.; Kanbara, T.; Shimura, M.; Kizu, K.; Maruyama, T.; Nakamura, Y.; Fukuda, T.; Lee, B.-L.; Ooba, N.; Tomaru, S.; Kurihara, T.; Kaino, T.; Kubota, K.; Sasaki, S. *J. Am. Chem. Soc.* **1996**, *118*, 10389.
- (26) (a) Watanabe, J.; Harkness, B. R.; Sone, M.; Ichimura, H. *Macromolecules* **1994**, *27*, 507. (b) Coates, G. W.; Dunn, A. R.; Henling, L. M.; Ziller, J. W.; Lobkovsky, E. G.; Grubbs, R. H. *J. Am. Chem. Soc.* **1998**, *120*, 3641.
- (27) When preparation of the polymer (PAE-4; cf. eq 4) was carried out at a lower temperature (e.g., room temperature) or short polymerization time (e.g., 6 h), only oligomeric products were obtained. These oligomeric products, oligomeric PAE-4, showed a $\pi-\pi^*$ absorption peak at 405 nm in solutions. Elongation of the polymer chain seems to bring about not only expansion of the π -conjugation system in the single PAE-4 molecule but also stacking of the long PAE-4 molecules. The stacking force between regioregular head-to-tail-type poly(3-alkylthiophene) molecules increases with increases in the molecular weight of the polymer.^{11f}
- (28) (a) van Hutten, P. F.; Wildeman, J.; Meetsma, A.; Haziioannou, G. *J. Am. Chem. Soc.* **1999**, *121*, 5910. (b) Tokito, S.; Saito, S.; Tanaka, R. *Makromol. Chem. Rapid. Commun.* **1986**, *7*, 557.
- (29) (a) Paker, V. D. *Electrochim. Acta* **1973**, *18*, 519. (b) Bard, A. J.; Lund, H., Ed. *Encyclopedia of Electrochemistry of the Elements*; Marcel Dekker: New York, 1978; XI 272; 1978; XII, 198. (c) Paker, V. D.; Ebersson, L. *J. Chem. Soc. Chem. Commun.* **1970**, 1289. (d) Hydroquinone in DMF (0.1 M $[\text{NEt}_4]\text{BF}_4$) gives the CV peaks (at 0.41 V (E_1), 0.85 V (E_2), -0.77 (E_3), and -1.34 V (E_4)) at almost the same position as hydroquinone in CH_3CN .^{29a–c}
- (30) At faster scanning velocity (e.g., 200 mV s^{-1}), both the CV curves of hydroquinone and PPP-2,5-OH give the E_5 peak (at about -1.35 V and -1.30 V vs Ag/Ag^+ for hydroquinone and PPP-2,5-OH, respectively) more clearly in the DMF solution (cf. CV charts in Supporting Information). An additional anodic peak E_6 (at about -0.8 V vs Ag/Ag^+ for the both) is also observed at the faster scanning velocity. The E_5 and E_6 may be assigned to n -undoping processes (or oxidation) of $[\text{NBu}_4]\text{Q}^{2-}$ and $[\text{NBu}_4]\text{Q}^{\cdot-}$ partly formed at the E_4 and E_3 processes, respectively. At the faster scanning velocity, the acceptance of H^+ by the reduced species $\text{Q}^{\cdot-}$ (eq 11) will not proceed smoothly in the anhydrous DMF solution, and $[\text{NBu}_4]\text{Q}^{\cdot-}$ and $[\text{NBu}_4]_2\text{Q}^{2-}$ seem to be partly formed in addition to HQ^{\cdot} and H_2Q (eqs 11 and 12), respectively.
- (31) (a) Peover, M. E.; Davies, J. D. *J. Electroanal. Chem.* **1963**, *6*, 46. (b) Audebert, P.; Bidan, G. *J. Electroanal. Chem.* **1987**, *238*, 183.
- (32) (a) Lide, D. R., Ed. *CRC Handbook of Chemistry and Physics*, 76th ed.; CRC Press: Boca Raton, 1995; p. 10–186. (b) Yamamoto, T. *J. Polym. Sci.: Part A: Polym. Chem.* **1996**, *34*, 997 and references therein.
- (33) (a) Steinberg-Yfrach, G.; Rigaud, J.-L.; Durantini, E. N.; Moore, A. L.; Gust, D.; Moore, T. A. *Nature* **1998**, *329*, 479. (b) Nichols, J. W.; Hill, M. W.; Bangham, A. D.; Deamer, D. W. *Biochim. Biophys. Acta* **1980**, *596*, 393. (c) Prabhananda, B. S.; Kombrabail, M. H. *Biochim. Biophys. Acta* **1988**, *1370*, 41. (d) Nojima, S.; Sunamoto, J.; Inoue, K., Eds. *The Liposomes*; Nankodo: Tokyo, 1988; p. 130. (e) Rabinowitz, J. D.; Vacchino, J. V.; Beeson, C.; McConnell, H. M. *J. Am. Chem. Soc.* **1998**, *120*, 2464.
- (34) (a) Miller, L. L.; Mann, K. R. *Acc. Chem. Res.* **1996**, *29*, 417. (b) Winokur, M. J.; Wamsley, P.; Moulton, J.; Smith, P.; Heeger, A. J. *Macromolecules* **1991**, *24*, 3812. (c) Yang, C.; Orfino, F. P.; Holdcroft, S. *Macromolecules* **1996**, *29*, 6510.
- (35) (a) Jordan, E. F., Jr.; Feldeisen, D. W.; Wrigley, A. N. *J. Polym. Sci., Part A-1* **1971**, *9*, 1835. (b) Hsieh, H. W.; Post, B.; Morawetz, H. *J. Polym. Sci.; Polym. Phys. Ed.* **1976**, *14*, 1241.
- (36) Salaneck, W. R.; Clark, D. T.; Samuelsen, E. J., Eds. *Science and Applications of Conducting Polymers*; Adam Hilger: Bristol, 1991.
- (37) Lidzey, D. G.; Alvarado, S. F.; Seidler, P. F.; Bleyer, A.; Bradley, D. D. C. *Appl. Phys. Lett.* **1997**, *71*, 2008.
- (38) (a) Bogdanovic, B.; Kröner, M.; Wilke, G. *Justus Liebigs Ann. Chem.* **1966**, *699*, 1. (b) Coulson, D. R. *Inorg. Synth.* **1972**, *13*, 121.
- (39) Vahlenkamp, T.; Wegner, G. *Macromol. Chem. Phys.* **1994**, *195*, 1933.
- (40) Noland, W. E.; Bande, F. J. *J. Org. Chem.* **1966**, *31*, 3321.
- (41) Kallitsis, J. K.; Gravalos, K. G.; Hilberer, A.; Hadziioannou, G. *Macromolecules* **1997**, *30*, 2989.
- (42) *International Tables for X-ray Crystallography*, Vol. IV; Kynoch: Birmingham, U.K., 1974.